Supporting information for:

Structure Determination and Interception of Biosynthetic Intermediates for the Plantazolicin Class of Highly Discriminating Antibiotics

Katie J. Molohon, Joel O. Melby, Jaeheon Lee, Bradley S. Evans, Kyle L. Dunbar, Stefanie B. Bumpus, Neil L. Kelleher, Douglas A. Mitchell*

Table of contents:

Methods

Production and purification of PZN. Overnight cultures (4 x 20 mL) of *B. amyloliquefaciens* FZB42 strain RSpMarA2 (Δ*sfp, yczE, degU*) (*8*) were used to inoculate 4 x 6 L flasks with 2 L of Luria Burtani (LB) broth supplemented with chloramphenicol (7 μg mL^{-1}) and kanamycin (7 μg mL^{-1}). Cultures were grown with shaking for 48 h at 37 °C. Cells were harvested by centrifugation (4,000 x *g*), washed with Tris-buffered saline (pH 8.0), and harvested a second time. Crude PZN was obtained by a non-lytic, methanolic extraction of the cellular surface. Cells were resuspended in MeOH (10% culture volume) and anhydrous Na_2SO_4 (5 g/L culture). The cell mixture was agitated by vortex (45 s) and equilibrated for 15 min at 22 °C. The supernatant was retained after centrifugation (4,000 x *g*), vacuum filtered with Whatman filter paper, and rotary evaporated to dryness to yield about 100 mg/L of a yellowish-brown solid. This crude material was dissolved in 80% aqueous MeCN (10 mL for 8 L culture), where the sample separated into two layers. The top organic layer was retained and concentrated for injection onto an Agilent 1200 series liquid chromatograph that was fitted inline to an Agilent 6100 Series Quadrupole LC/MS. For preparative purposes, PZN was reverse phase purified using a Thermo BETASIL C18 column (250 mm x 10 mm; pore size: 100 Å; particle size: 5 μm) at a flow rate of 4 mL min^{-1}. A gradient of 65-85% MeOH with 0.1% formic acid over 32 min was used. The fractions containing PZN (as monitored by A_{266} and MS) were collected into 20 mL borosilicate vials and the solvent removed *in vacuo*. The isolated yield for PZN following this procedure was routinely 150-200 μg L^{-1} culture. Mutant RS33 (Δ*sfp*, *bac*, *pznL*) was prepared similarly, with the only exceptions being a 24 h fermentation, substitution of spectinomycin (90 μg mL^{-1}) for kanamycin, and elimination of the TBS wash.

Production of PZN (elevated oxygen). Increased aeration of *B. amyloliquefaciens* FZB42 strains RSpMarA2 and RS33 were achieved using a New Brunswick Scientific BioFlo 110 Fermenter system. RSpMarA2 and RS33 (9 L) were cultured at 37 °C with 250 rpm stirring for 24 h. Air was

supplied at 5 L/min (saturated in oxygen, ~1 L min^{-1}).

On-line RPLC-FTMS. All reverse phase liquid chromatography (RPLC)-Fourier-transform mass spectrometry (FTMS) was conducted using an Agilent 1200 high performance LC (HPLC) system with an autosampler coupled directly to a ThermoFisher Scientific LTQ-FT hybrid linear ion trap-FTMS system operating at 11 tesla. The MS was calibrated weekly using the calibration mixture and instructions specified by the manufacturer. All instrument parameters were tuned according to the manufacturer's instructions (employing bovine ubiquitin for tuning purposes). For all analyses of PZN, a 1 mm x 150 mm Jupiter C18 column (Phenomenex, 300 Å, 5 μm) was connected in-line with the electrospray ionization source (operated at ~5 kV with a capillary temperature of 200-250 °C) for the MS system. A typical sample was loaded onto the column using the autosampler and separated using a linear gradient of H_2O/MeCN and 0.1% formic acid with the analytes eluted directly into the MS. All ionized species were subjected to an MS method with five MS and MS/MS events: 1) full scan measurement of all intact peptides (all ions detected in the FTMS in profile mode; resolution: 100,000; *m/z* range detected: 400-2000), 2-5) data-dependent MS/MS on the first, second, third, and fourth most abundant ions from scan (1) using collision induced dissociation (CID) (all ions detected in the FTMS in profile mode; minimum target signal counts: 5,000; resolution: 50,000; *m/z* range detected: dependent on target *m/z*, default charge state: 2, isolation width: 5 *m/z*, normalized collision energy: 35; activation q value: 0.40; activation time: 30 ms). During all analyses, dynamic exclusion was enabled with the following settings: repeat count – 2, repeat duration – 30 s, exclusion list size – 300, exclusion duration – 60 s.

Direct infusion FTMS. After lyophilization for at least 24 h, HPLC purified samples were dissolved in 80% MeOH (to ~0.5 mg mL^{-1}) and then further diluted 10-fold into 50% MeOH supplemented with 0.1% (v/v) formic acid. The diluted samples were directly infused using an Advion Nanomate 100.

The singly charged ions were targeted for CID using identical settings as above, except that the resolution was set to 100,000.

N-terminal labeling. Purified PZN and desmethylPZN were dissolved in 80% MeCN, 10 mM MOPS (pH 8.0) to a final concentration of 1.5 mM. An aliquot (5 µL) was transferred to a microfuge tube containing 5 µL of 80% MeCN, 10 mM MOPS (pH 8.0) supplemented with 20 mM EZ-Link® sulfo-NHS-biotin. Control reactions lacked the NHS-biotin reagent. The samples were allowed to react for 3 h at 23 °C prior to analysis on an Applied Biosystems Voyager DE-STR MALDI-TOF-MS.

NMR. PZN was produced from low oxygenation cultures and purified as described in the main text methods. PZN (700 µg) was dissolved in 200 µL of DMSO-d_6 and placed into an Advanced Shigemi 5 mm NMR tube matched to DMSO-d_6. NMR experiments were conducted on a Varian Unity Inova 500 NB (^{1}H-^{1}H-gCOSY) and a Varian Unity Inova 600 spectrometer (^{1}H, ^{1}H-^{1}H-TOCSY and ^{1}H-^{13}C-gHMBC) using a 5 mm Varian ^{1}H{^{13}C/^{15}N} PFG Z probe and 5 mm Varian ^{1}H{^{13}C/^{15}N} XYZ PFG triple resonance probe, respectively. The ^{1}H-NMR, TOCSY and gHMBC experiments were conducted at 25 °C and utilized water suppression. A mixing time of 150 ms was used for the TOCSY. For the gHMBC, ^1J and ^nJ were set to 140 and 8 Hz, respectively. Chemical shifts were referenced using DMSO (δ_H=2.50 and δ_C=39.51), and the spectra were processed and analyzed using MestReC. Stereochemical configuration was assumed to be identical to the ribosomally produced precursor peptide.

Determination of MIC. *B. anthracis* strain Sterne was grown to stationary phase in a 10 mL LB culture at 37 °C. The culture was adjusted to OD_{600} of 0.01 in LB broth and added to 96-well plates. 2-fold dilutions of PZN (5 mg mL^{-1} in 80% MeCN) were added to the cultures (0.5 – 128 µg mL^{-1}). Kanamycin was added similarly to control samples, with dilutions from 1 – 32 µg mL^{-1}. Covered

plates were incubated at 37 °C for 12 h. The minimum inhibitory concentration that suppressed the growth of at least 99% of the bacteria (MIC_{99}) was established based on culture turbidity. Additional pathogens were grown and prepared similarly as above, with the exception of optimizing the growth media to match an organism's nutritional requirements (*Streptococcus pyogenes*, Todd Hewitt broth; *Listeria monocytogenes*, *Enterococcus faecalis* st. U503 [VRE], and *Staphylococcus aureus* st. NRS384/USA300 [MRSA], brain heart infusion). Positive controls: *S. pyogenes* and *L. monocytogenes*, kanamycin; *E. faecalis*, tetracycline; *S. aureus*, vancomycin. Bactericidal activity was determined by diluting 1 μL of *B. anthracis* strain Sterne grown with 8 μg mL^{-1} PZN into 99 μL of media. The sample was then streaked onto LB agar plates and incubated for 24 h for counting colony-forming units.

Agar diffusion bioassay. *B. anthracis* strain Sterne was grown as described previously and diluted to OD_{600} of 0.13. The diluted culture (100 μL) was inoculated onto an LB plate and allowed to dry. HPLC-purified PZN (50-200 μg) was added to a paper disk, dried, and added to the plate. Culture were then incubated at 37 °C for 12 h. Kanamycin (8-25 μg) was used as a positive control, and 80% MeCN was the negative (solvent) control.

Microscopy. Differential interference contrast (DIC) microscopy images were obtained by preparing live cell images of *B. anthracis* cultures. Samples were pretreated with or without PZN at 4 μg mL^{-1} (MIC_{99}) and morphology was assessed using a Zeiss LSM 700 microscope. The objective used was a Plan-Apochromat 63x/1.40 Oil DIC M27. The analysis software used was Program Zen 2009 Light Edition.

Production of PZN from Bacillus pumilus ATCC 7061. Cultures were prepared as described above, but with the exception no antibiotics were added. The method employed for metabolite extraction

and HPLC purification were identical to samples from *B. amyloliquefaciens*. Purified fractions were analyzed on a Bruker Daltonics ultrafleXtreme MALDI-TOF/TOF instrument operating in reflector/positive mode. Sinapic acid was used as the matrix.

Figure S1:

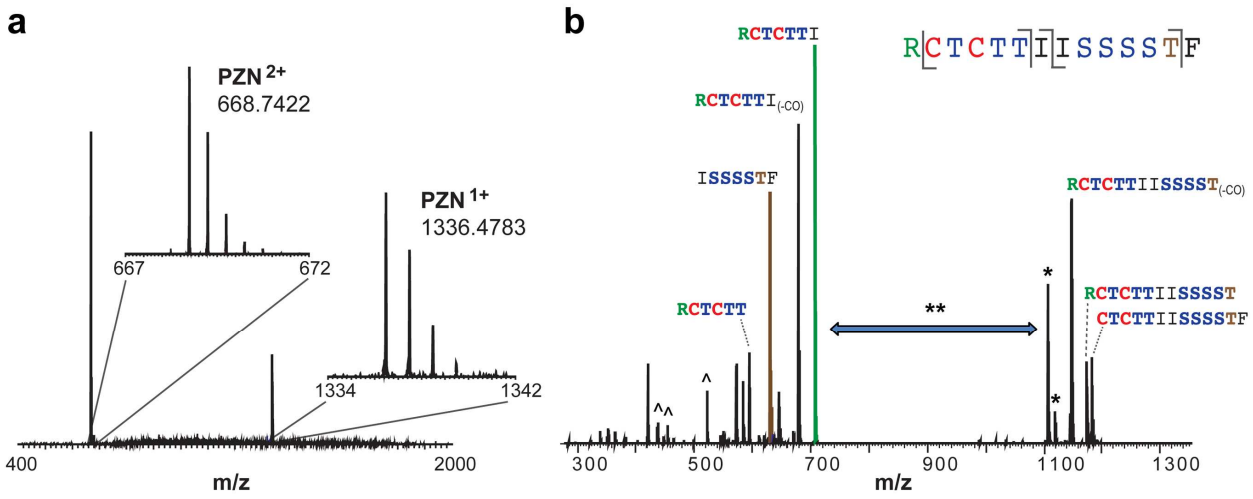

A, Broadband spectrum of HPLC-purified PZN on a linear ion trap MS (11 Tesla LTQ-FT). Visible are the singly and doubly charged positive ions of PZN. Due to the high mass accuracy of FT-MS (<5 ppm error) and the known sequence of the precursor peptide (*1, 2*), the molecular formula of PZN was deduced from this mass measurement. This formula required that 9 out of the 10 heterocyclizable residues were converted to the azole heterocycle and the remaining residue was left at the azoline oxidation state. Also, this formula required two methylation events (consistent with earlier deletion studies) and leader peptide cleavage after Ala-Ala (see Figure 4b). **B**, Collision induced dissociation (CID) spectrum of *m/z* 668.7 (PZN^{2+}). The fragmentation pattern of PZN in the doubly charged state is markedly different than that of the singly charged species shown in Figure 1b of the main text. The amino acid sequence for the PZN precursor peptide from *B. amyloliquefaciens* FZB42 (BamA) is color-coded by posttranslational modification as follows: N^{α},N^{α}-dimethylarginine (green), thiazoles (red), methyloxazoles and oxazoles (blue), and methyloxazoline (brown). Identified fragment ions are also plotted onto the BamA precursor sequence. The most diagnostic peaks for localizing posttranslational modifications resulted from Ile-Ile cleavage (green and brown mass peaks). These ions demonstrate that both methylation events are on the N-terminal fragment and that the sole azoline moiety is on the C-terminal fragment. *****Fragment ions with the azoline as the most C-terminal moiety spontaneously decompose, supporting the assignment of the C-terminal Thr as being converted to methyloxazoline in PZN (assigned in Figure S3). Under the CID conditions employed, most peptides will fragment at the amide bond. The first step in TOMM biosynthesis, cyclodehydration, removes an amide bond from the peptide backbone. ******Contiguous heterocycles thus preclude the formation of a complete series of y^{+} and b^{+} ions and results in a CID spectrum that is featureless from *m/z* ~710-1100. One non-amide cleavage is noted between arginine and cysteine (highest mass ion in the spectrum), which permits the methyl groups to both be localized to arginine. **^**Internal fragments (assigned in Figure S3).

Figure S2:

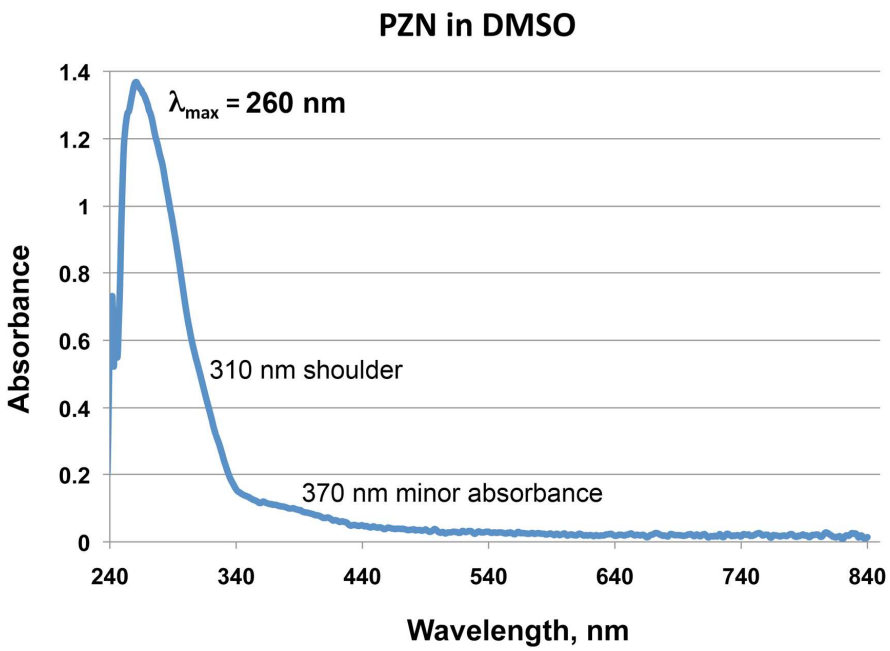

UV-Vis spectrum of HPLC-purified PZN in DMSO acquired on a Nanodrop 2000. The instrument was blanked on DMSO, which has a UV cut-off of approximately 245 nm. The extinction coefficient for PZN in DMSO is ε_{260} = 560 $M^{-1}cm^{-1}$. The λ_{max} in 80% acetonitrile/water is 266 nm.

Figure S3:

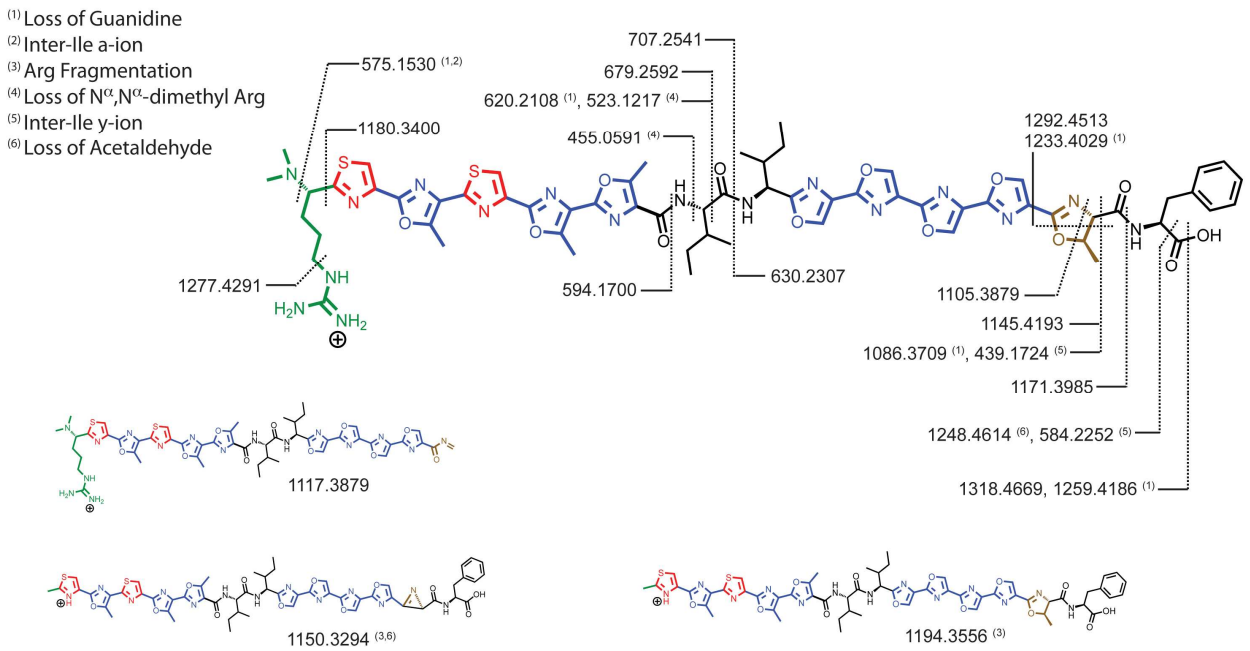

Observed fragments during MS/MS of PZN (*m/z* 1336). Cleavage sites are shown with their corresponding theoretical monoisotopic fragment masses. Some of the observed fragments are derived from multiple bond cleavages, denoted by superscripts (these are not intended to suggest a pathway of fragmentation). In the lower part of the figure, structures with more complex fragmentation pathways are shown with their corresponding masses. The *m/z* 1277 structure permits the localization of both methyl groups to the N-terminus of PZN. The *m/z* 1145 structure results from the loss of the C-terminal Phe residue and CO. In conjunction with selective hydrolysis studies, *m/z* 1145 and the subsequent azoline decomposition ions (1117 and 1105) localize the sole azoline as the C-terminal Thr residue. Further, we note many examples of neutral loss of acetaldehyde (C_2H_4O, exact mass = 44.0262; not to be confused with loss of CO_2, exact mass = 43.9898; >800 ppm difference). See the main text for an explanation of the formation of these ions.

Figure S4:

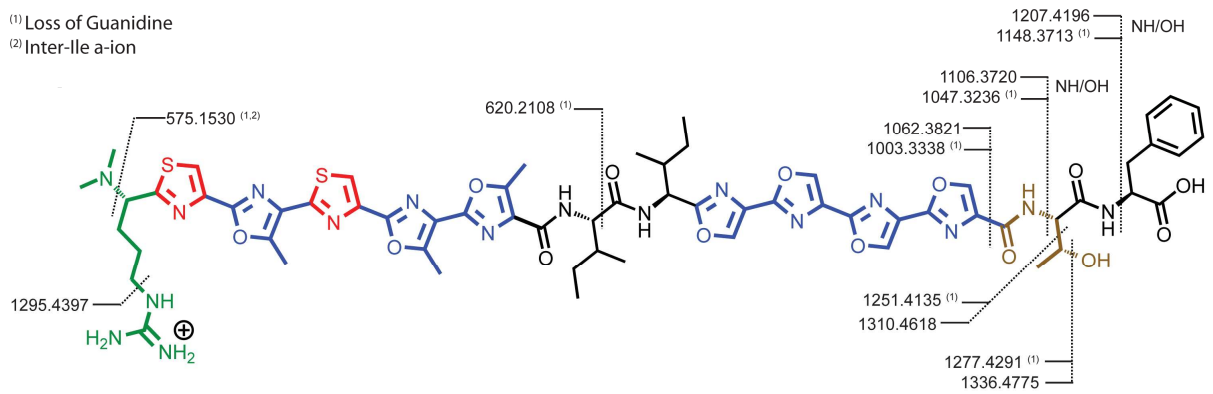

Observed fragments during MS/MS of hydrolyzed PZN (*m/z* 1354). Unlike their aromatic azole counterparts, azoline heterocycles are hydrolytically unstable in mild acid and mild base (*3*). Selective acidic hydrolysis of PZN was performed to convert the sole azoline heterocycle back to the original amino acid. This reinstates an amide bond that can be located by subsequent MS^n analysis. Observed cleavage sites are shown with their corresponding theoretical monoisotopic fragment masses. Some of the observed fragments are derived from multiple bond cleavages, denoted by superscripts (these are not intended to suggest multiple fragmentation events or a pathway of fragmentation). Note that upon methyloxazoline hydrolysis to threonine, in no cases can neutral loss of acetaldehyde be found. This implies that loss of acetaldehyde (formation of azirine) is specific to methyloxazolines under the CID conditions we employed. Note that loss of C_2H_4O is possible from hydrolyzed (Thr-containing) PZN, but only via dehydration and subsequent loss of acetylene. Other fragment ions of interest in this map confirm the site of dimethylation to be the N-terminal amine.

Figure S5:

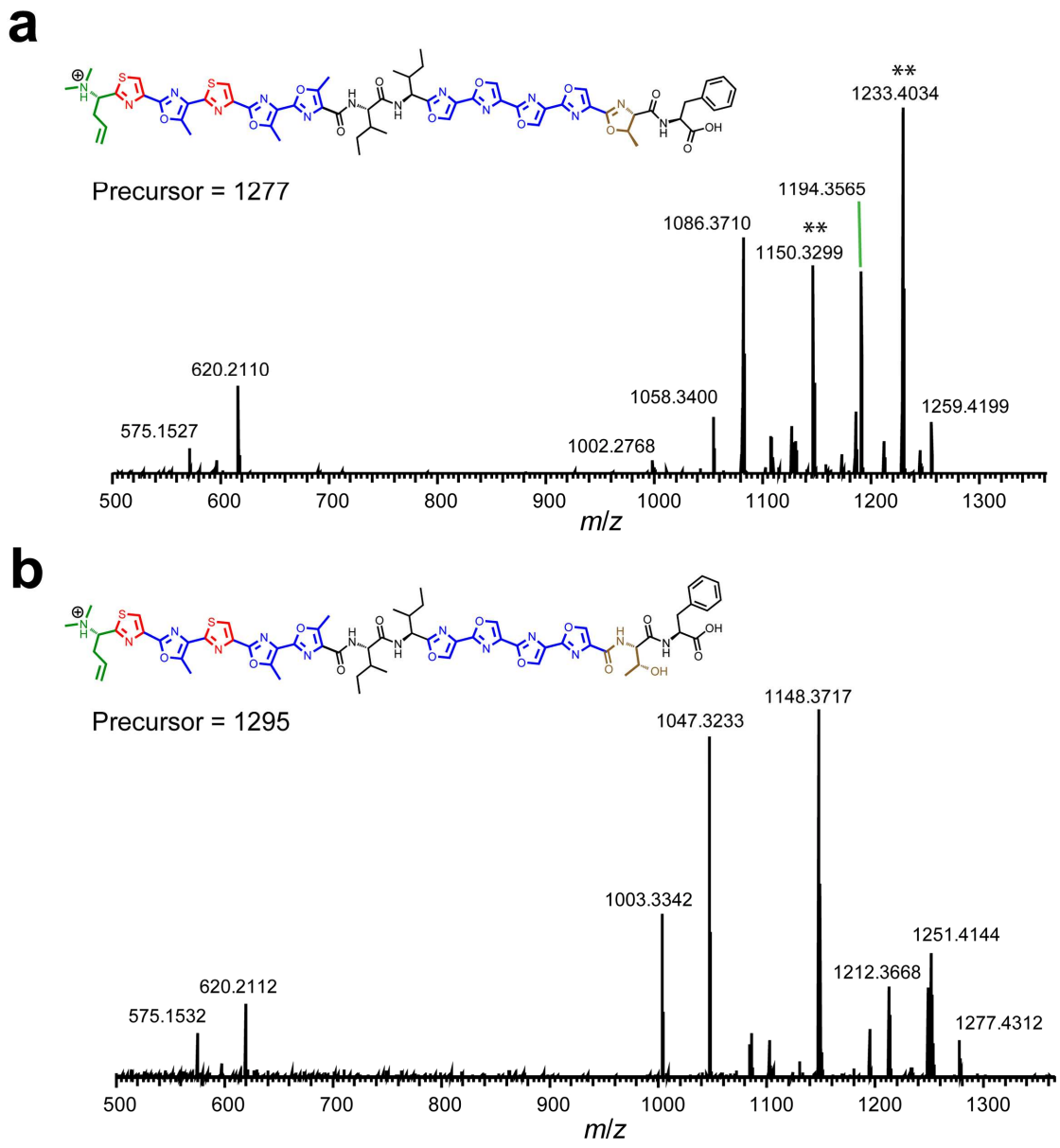

MS^3 collision induced dissociation (CID) spectra for **A**, deguanidinated PZN (*m/z* 1277) and **B**, deguanidinated hydrolyzed PZN (*m/z* 1295). **Indicates loss of acetaldehyde (44.0262 Da) from methyloxazoline (1277 – 44 = 1233; 1194 – 44 = 1150). Note that this is only possible in panel A, where an intact heterocycle is found. The ions at m/z 575, 1150, and 1194 demonstrate that the Arg was dimethylated on the amino terminus. Structural assignments are given for the fragments of deguanidinated PZN and deguanidinated hydrolyzed PZN in Figure S3 and S4, respectively.

Figure S6:

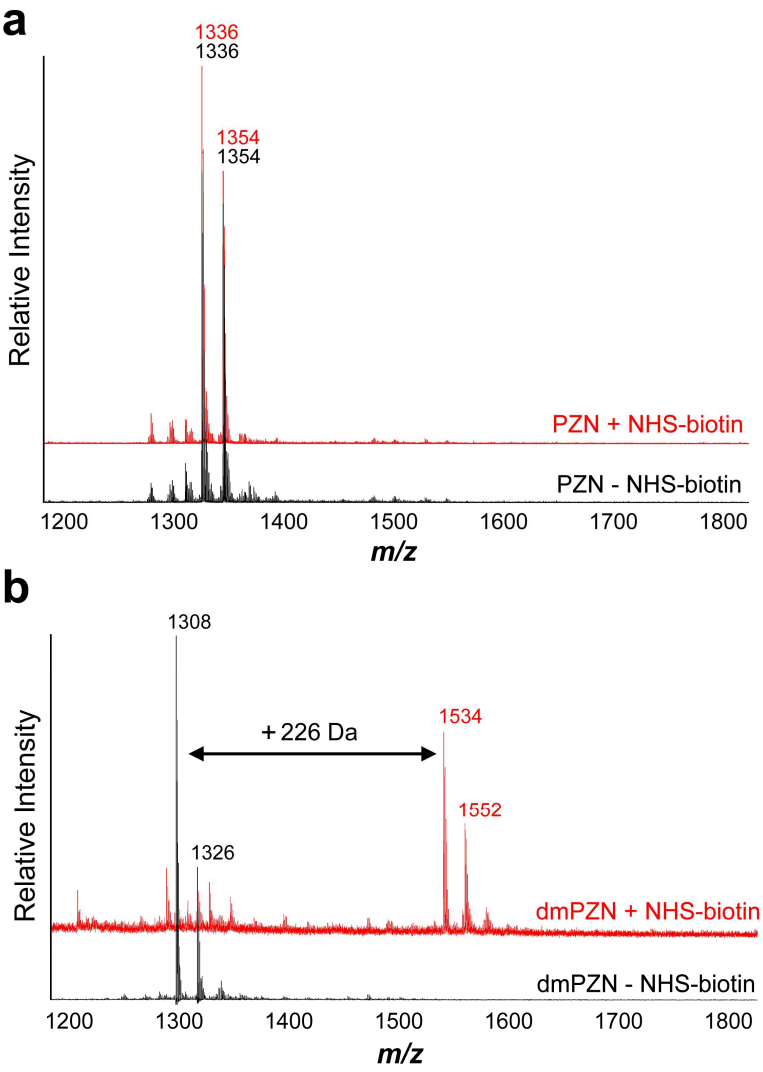

MALDI-TOF-MS results of NHS-biotin labeling for **A**, PZN (*m/z* 1336) and hydrolyzed PZN (*m/z* 1354) and **B**, desmethylPZN (*m/z* 1308) and hydrolyzed desmethylPZN (*m/z* 1326). Abbreviation: desmethylPZN, dmPZN. Red traces are samples that included the NHS-biotin reagent while black traces are from control reactions that lacked NHS-biotin. Labeling was only observed with desmethylPZN, as indicated by the new species at *m/z* 1534 and 1552. Addition of biotin gives a net mass increase of 226 Da ($C_{10}H_{14}N_2O_2S$). Specific labeling reactions are given in the methods section.

Table S1. Complilation of NMR results. Abbreviations: Tz, thiazole; Oz, oxazole; Ozn, oxazoline.

Amino acid	Position	δ_H (J in Hz)	^{1}H-^{1}H-gCOSY	^{1}H-^{1}H-TOCSY	^{1}H-^{13}C-gHMBC
Arg[1]	α	3.93; t (6.2)		1.53, 1.85, 1.96,	
	β	1.52; m		3.93, 1.85, 1.98	
	γ	0.87, 1.23; m			24.4, 36.8
	δ	1.86, 1.98; m		3.93	
	ε	n.d.			
	η1, η2	7.63, 7.72; m			
	N,N-dimet	2.26, s			65.6, 41.4
Tz[2]	5	8.41; s			
Me-Oz[3]	5-Met	2.81; s			147.2
Tz[4]	5	8.45; s			
Me-Oz[5]	5-Met	2.74; s			150.5
Me-Oz[6]	5-Met	2.63; s			152.3
Ile[7]	NH	7.88; s (10.2)	4.45	4.44, 0.86, 1.92	
	α	4.45; t (8.4)	1.93	7.88, 1.92, 0.86	
	β	1.93; m	4.45, 0.89	7.88, 4.45, 0.86, 0.81	
	γ^1	1.00; b			178.8
	γ^2	0.87; m	1.93	7.88, 1.93, 4.44	36.8, 56.7
	δ	0.81; m		1.93	22.2
Ile[8]	NH	8.78; d (7.8)	4.9	4.90, 0.84, 2.02	
	α	4.91; t (8.1)	8.8,2.1	8.78, 2.02, 0.84	
	β	2.05; m	4.9,0.85	8.78, 4.91, 0.88, 0.84	
	γ^1	1.00; b			
	$\gamma^{2\text{-met}}$	0.84; m	2.1	8.78, 2.02, 4.90	36.8, 51.3
	δ	0.88; m		2.02	22.6
Oz[9]	5	8.94; s			
Oz[10]	5	9.06; s			
Oz[11]	5	9.08; s			
Oz[12]	5	8.80; s			
Me-Ozn[13]	4	4.22; d (7.8)	4.61	4.6, 1.43	
	5	4.60; m	4.23, 1.44	4.21, 1.43	
	5-Met	1.44; d 6.6	4.61	4.6, 4.22	74.6, 79.5
Phe[14]	NH	7.17; d (7.8)	4.14	4.13, 3.00, 2.90	
	α	4.15; m	7.17, 3.00, 2.92	7.16, 3.00, 2.90	
	β	2.92, 3.02; d (5.4)	4.14	7.17, 4.14	
	δ^1, δ^2	6.94; m	7.02	7.06	125.6
	ε^1, ε^2	7.02; m	6.94	6.98	136.2
	ζ	6.98; m			

Figure S7:

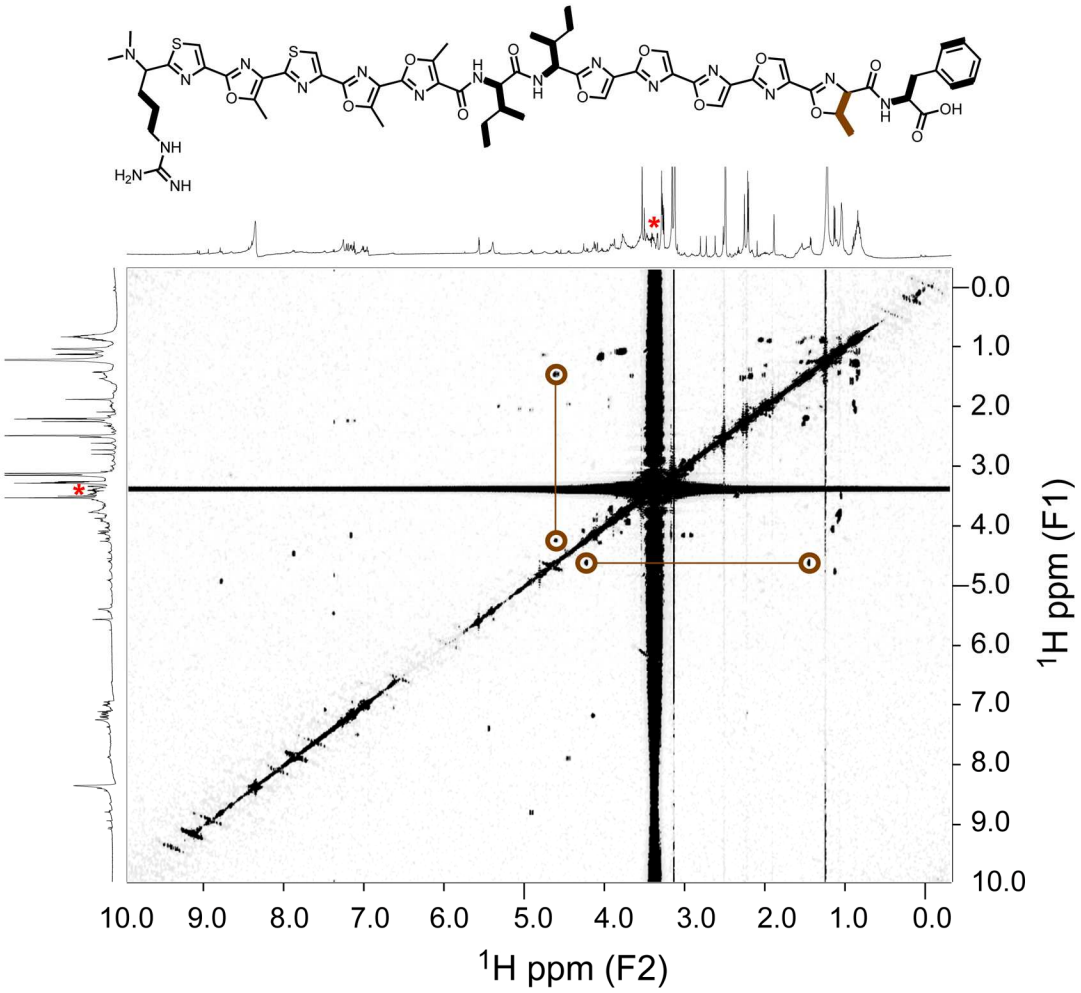

^{1}H-^{1}H-gCOSY of PZN. Assigned correlations are drawn on the structure of PZN as thickened bonds. The brown circles indicate correlations deriving from the methyloxazoline protons (shown as brown bonds in structure). The red asterisk indicates that in the 1D-^{1}H-spectrum, the signal from water was suppressed. This signal was not suppressed for the 2D experiment.

Figure S8:

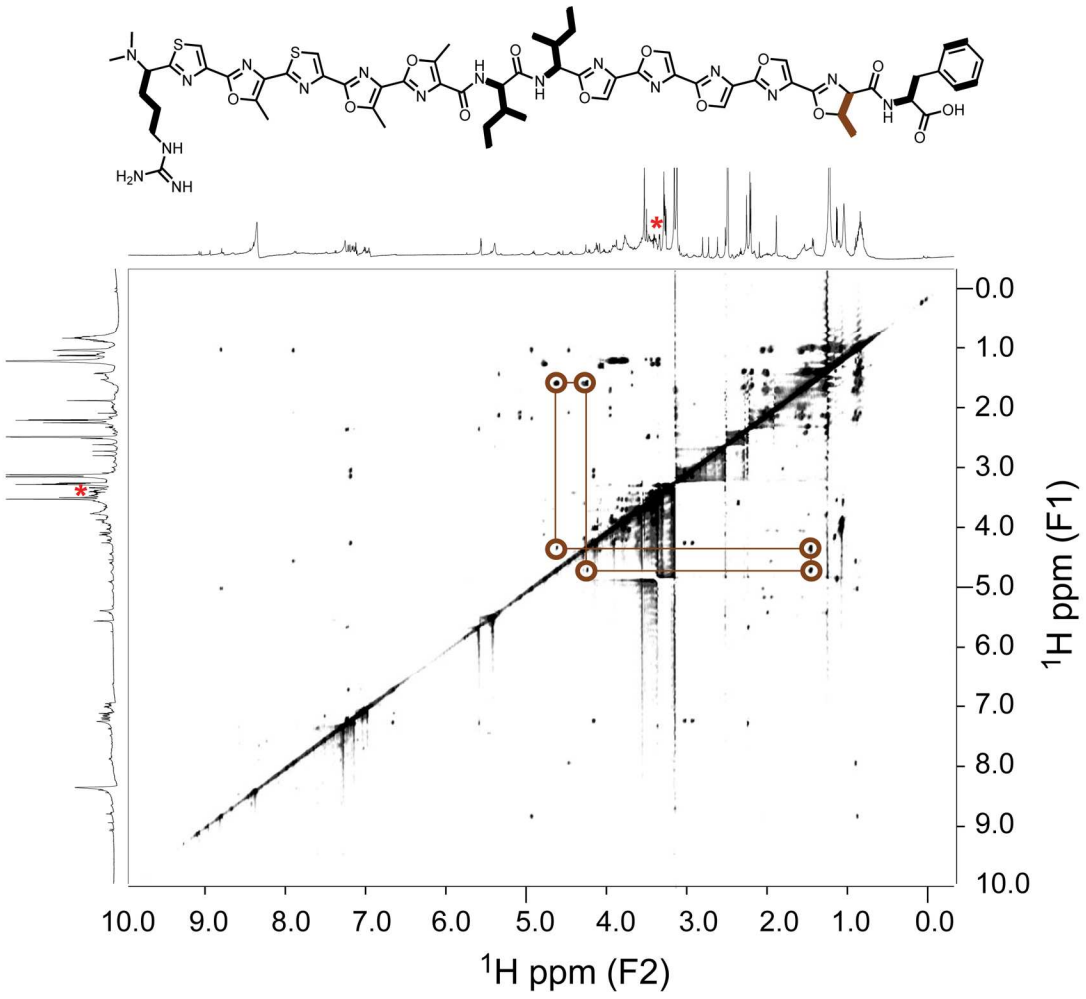

^{1}H-^{1}H-TOCSY of PZN. Assigned correlations are drawn on the structure of PZN as thickened bonds. The brown circles indicate correlations deriving from the methyloxazoline protons (shown as brown bonds in structure). The red asterisks on the 1D spectra indicate the signal from water suppression. This signal was also suppressed for the 2D experiment.

Figure S9:

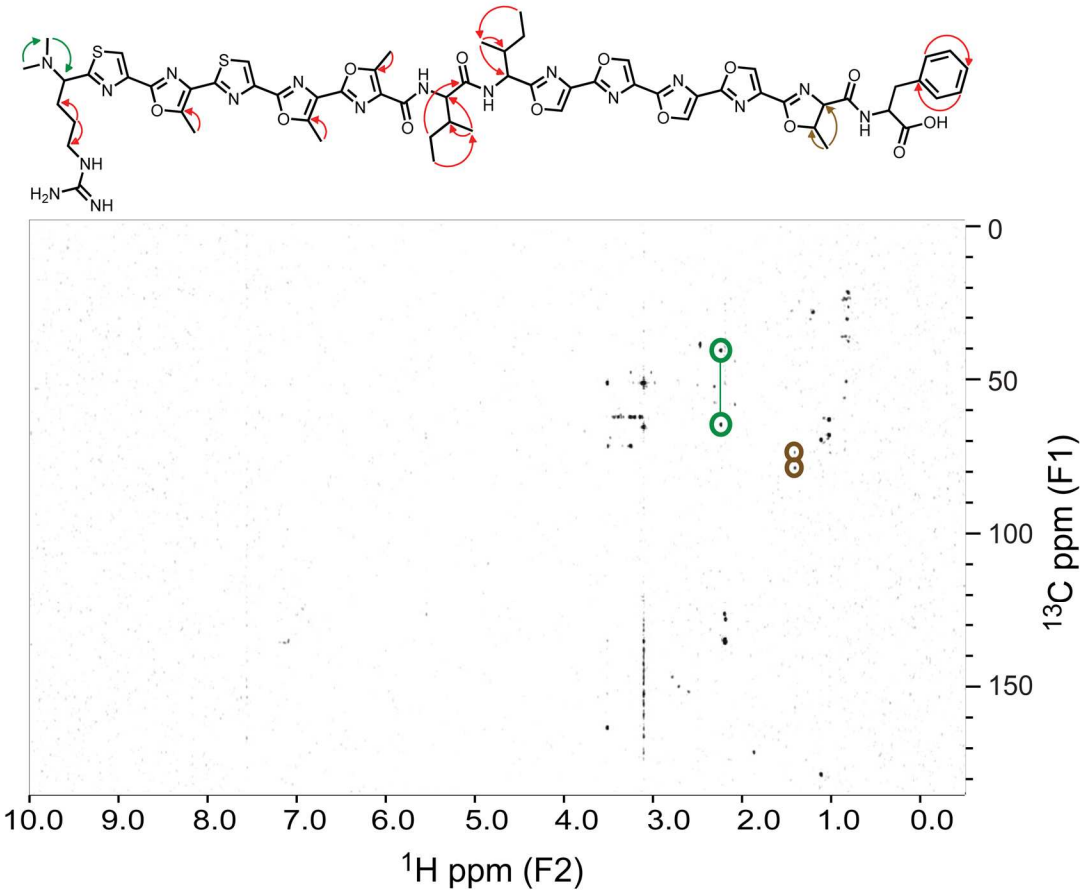

^{1}H-^{13}C-gHMBC of PZN. Assigned correlations are drawn on the structure of PZN as red arrows. The green arrows/circles indicate correlations that localize the posttranslational methyl groups to the N-terminus. The brown arrows/circles indicate correlations that demonstrate the azoline is methyloxazoline.

Figure S10:

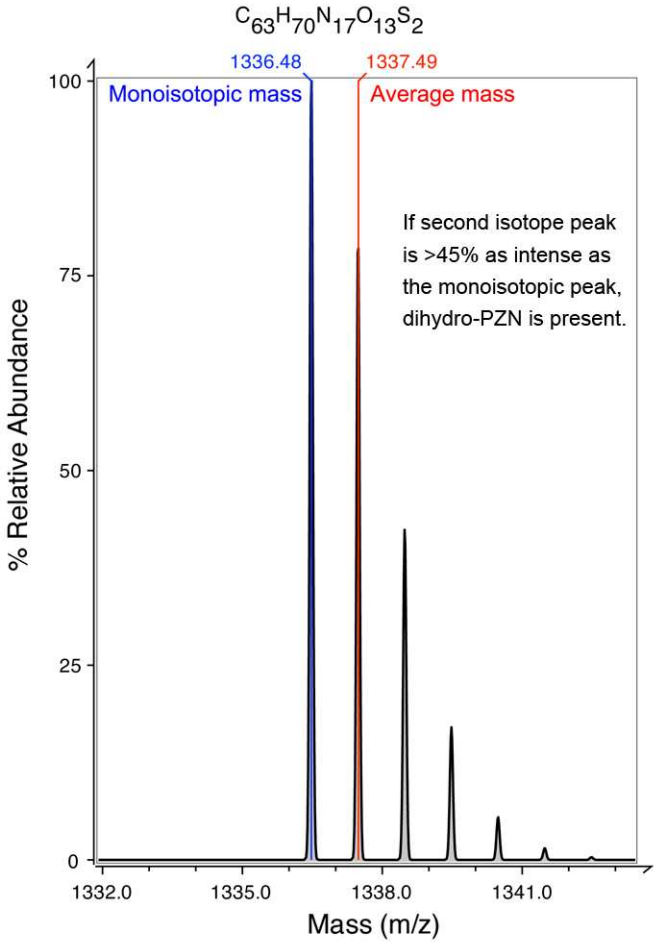

Predicted isotope pattern for PZN (*m/z* 1336). Note that the average mass is slightly heavier than the first isotope mass. This figure was generated using iMass version 1.1 (freeware written by Urs Roethlisberger).

Figure S11:

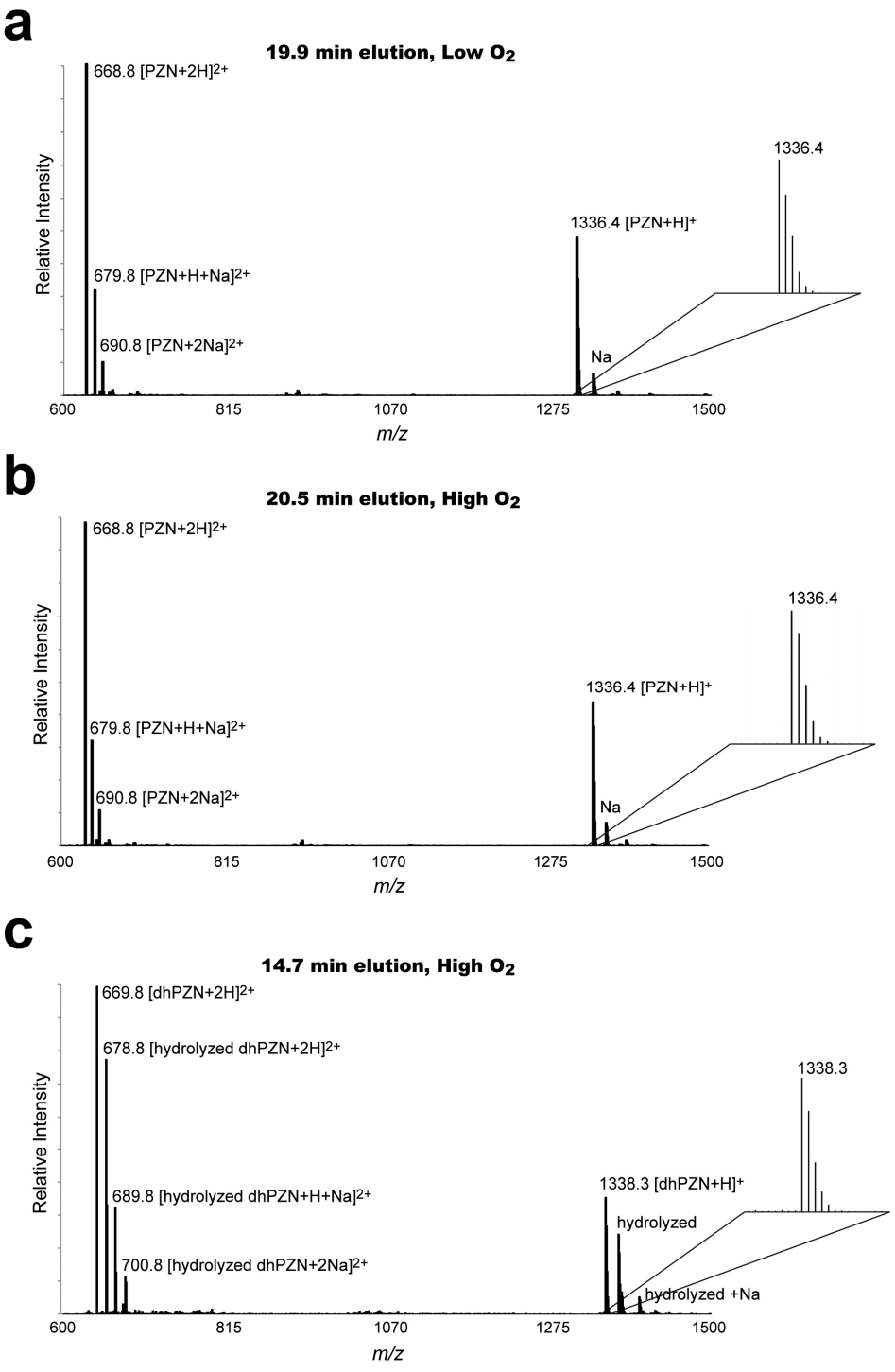

Effect of oxygen levels during fermentation on the production of PZN. ESI-MS at selected time points from LCMS analysis (UV, TIC, EIC) shown in Figure 2. **A**, Under low oxygen conditions, PZN (*m/z* 1336) is the only species present in the 19.9 min elution. **B**, Under an oxygen saturated fermentation, PZN is found in the 20.5 min elution. **C**, As expected from the EIC's shown in Figure 2, high oxygen fermentation yields an additional compound eluting at 14.7 min consistent with dihydroPZN (dhPZN, *m/z* 1338). The earlier elution of dhPZN relative to PZN is in agreement with azolines being more hydrophilic and basic than azoles (azoles are not protonated with 0.1% formic acid). Right insets for all panels show a zoomed in spectrum to highlight the isotopic pattern of the singly charged PZN species.

Figure S12:

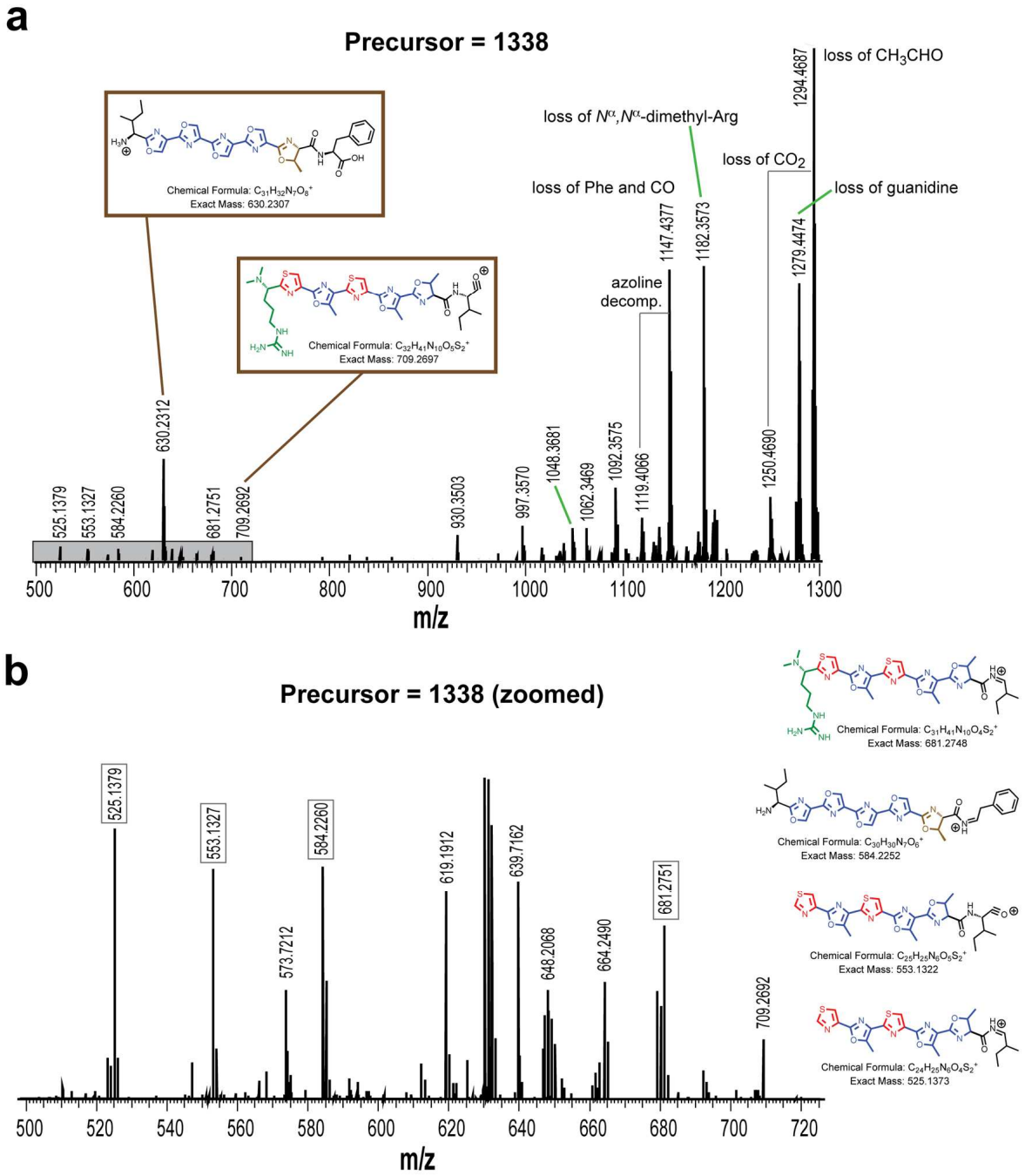

Partial localization of the second azoline in dihydroPZN (dhPZN). **A**, CID spectrum of dhPZN (*m/z* 1338) acquired using LTQ-FT-MS. The heavier fragment ions are identical to those shown in Figure 1 of the main text, with the exception of each fragment being 2 Da heavier. The gray box depicts a zoomed in region shown in panel B. Brown boxes highlight two ions demonstrating that an azoline heterocycle exists on each side of the Ile-Ile. The location of the C-terminal azoline was localized to the most C-terminal Thr. The location of the N-terminal azoline is likely to be the Thr adjacent to Ile due to similar sterics/electronics. However, the precise position cannot be concluded from this spectrum. **B**, Zoomed in region from panel A (gray box). Diagnostic ions are boxed in gray and their respective (predicted) structures drawn in the right margin.

Figure S13:

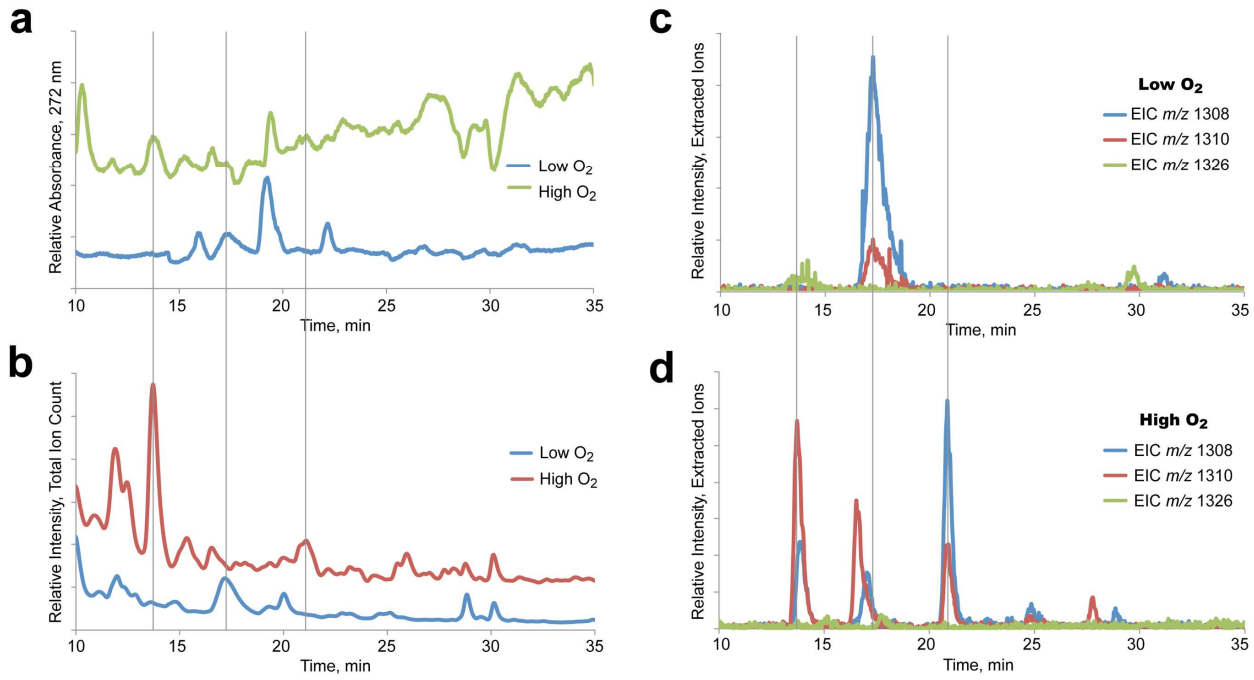

Effect of oxygen levels during fermentation on the production of desmethylPZN. In each case presented, the low oxygen samples were prepared by shake flask fermentation of *B. amyloliquefaciens* strain RS33 (*pznL* deletion, desmethylPZN producer) in 2 L of LB in 6 L flasks. High oxygen samples were prepared using a biofermentor with 5 L/min air input. Both cultures were grown for 24 h at 37 °C. All samples were extracted in an identical fashion and subjected to identical chromatographic procedures (analytical C_{18}-HPLC) as described in the methods. In all panels, vertical lines are drawn at 14, 17, and 21 min. **A**, UV chromatogram (Abs 272 nm) of RS33 extract from high and low oxygen fermentation. This trace shows that more chromophores absorbing light at 272 nm are produced under high oxygen conditions. **B**, Same as A except the trace is the total ion chromatogram (TIC). **C**, Extracted ion chromatogram (EIC) of *m/z* 1308, 1310, and 1326 from low oxygen fermentation. Under these conditions, the majority species is desmethylPZN (1308) with trace amounts of hydrolyzed desmethylPZN (1326). The 1310 trace that appears to "coelute" with 1308 at 17 min is the actually the second isotope peak of 1308, not dihydrodesmethylPZN (see Figure S10). **D**, Same as C except under high oxygenation conditions. The peaks at 14 and 16 min contain primarily dihydrodesmethylPZN (*m/z* 1310) while the peaks at 17 and 21 min contain primarily desmethylPZN (*m/z* 1308). The species eluting at 14 and 16 min are suspected to be regioisomers, as are the species eluting at 17 and 21 min. ESI-MS at these selected time points are shown in Figure S14.

Figure S14:

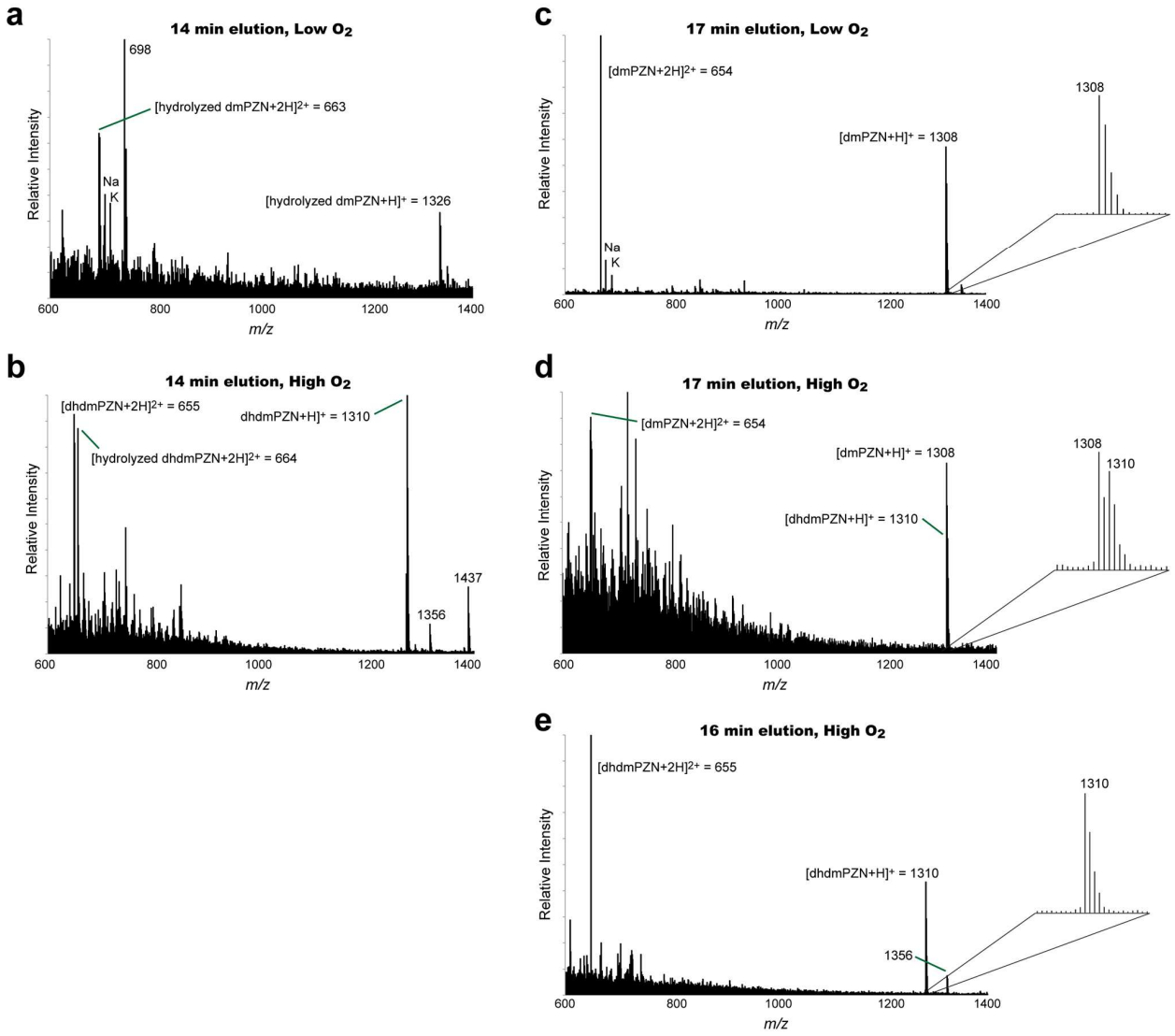

Effect of oxygen levels during fermentation on the production of desmethylPZN. ESI-MS at selected time points from LCMS analysis (UV, TIC, EIC) shown in Figure S13. **A**, Under low oxygen conditions, hydrolyzed desmethylPZN (*m/z* 1326) is visible in the 14 min elution. **B**, As expected from the EIC's shown in Figure S13, the 14 min elution is dominated by dihydrodesmethylPZN (*m/z* 1310) at the 14 min elution. **C**, Low oxygen fermentation and an elution of 17 min yields exclusively desmethylPZN (*m/z* 1308). As indicated by the ion purity and signal to noise ratio in this spectrum, relative to the other panels, desmethylPZN was a majority product and easily separated under the conditions employed. **D**, Same as C but high oxygen conditions led to the production of a mixture of desmethylPZN and dihydrodesmethylPZN (ratio ~60:40, respectively). **E**, At 16 min under high oxygen conditions, 1310 is the majority species produced, consistent with azolines being more hydrophilic than azoles. Right insets for panels C-E show a zoomed in spectrum to highlight the isotopic pattern of the singly charged desmethylPZN species. The ratio of intensities given in Figure S10 applies.

Figure S15:

PznJ

	Bam	Bpum	Cms	Cur	Blin
Bam	100	63	26	6	10
Bpum	90.1	100	27	8	6
Cms	61.8	61.2	100	13	12
Cur	51.4	49.4	52.7	100	54
Blin	47.2	48.7	54.4	87	100

PznB

	Bam	Bpum	Cms	Cur	Blin
Bam	100	77	57	44	43
Bpum	96.3	100	57	43	42
Cms	87.5	87.1	100	43	42
Cur	78.8	81.3	77.1	100	86
Blin	77.3	78.8	76.7	98.2	100

PznC

	Bam	Bpum	Cms	Cur	Blin
Bam	100	63	41	22	25
Bpum	91.1	100	40	26	27
Cms	77	77.4	100	24	24
Cur	64	66.3	65.1	100	73
Blin	64.7	66.1	66.5	93.2	100

PznE

	Bam	Bpum	Cms	Cur	Blin
Bam	100	44	16	15	14
Bpum	78.1	100	13	13	13
Cms	54.6	56.1	100	20	18
Cur	55.5	48	50	100	52
Blin	49.5	55.9	49	83.7	100

PznD

	Bam	Bpum	Cms	Cur	Blin
Bam	100	82	57	38	38
Bpum	96.8	100	56	38	38
Cms	76	74.2	100	39	38
Cur	73	73.7	64.5	100	79
Blin	71.4	71.1	64	94.6	100

PznL

	Bam	Bpum	Cms	Cur	Blin
Bam	100	48	25	22	18
Bpum	81.6	100	25	21	18
Cms	60.3	59.2	100	20	22
Cur	55.7	54.4	54	100	53
Blin	57.4	54.4	50.5	87.6	100

Order of similarity:
PznB > PznD > PznC > PznL > PznJ > PznE

Order of identity:
PznB > PznD > PznC > PznL > PznJ > PznE

Similarity/identity matrix of related (PZN-producing) biosynthetic proteins. Shown in yellow are amino acid identity scores obtained by pairwise alignment using ClustalW2, which includes the standard parameters for gap penalties. In blue are the corresponding amino acid percent similarity values, obtained by recording the ratio of similar amino acids to the full protein sequence after alignment (no gap penalties). PznJ, required biosynthetic protein of unknown function; PznC, cyclodehydratase; PznD, docking protein; PznB, FMN-dependent dehydrogenase; PznE, suspected leader peptidase; PznL, SAM-dependent methyltransferase. Abbreviations used are derived from the genus and species name for each organism. Bam, *Bacillus amyloliquefaciens* FZB42; Bpum, *Bacillus pumilus* ATCC 7061; Cms, *Clavibacter michiganensis* subsp. *sepedonicus*; Cur, *Corynebacterium urealyticum* DSM 7109; Blin, *Brevibacterium linens* BL2. Bam and Bpum are Firmicutes, while the other three species are Actinobacteria.

Figure S16:

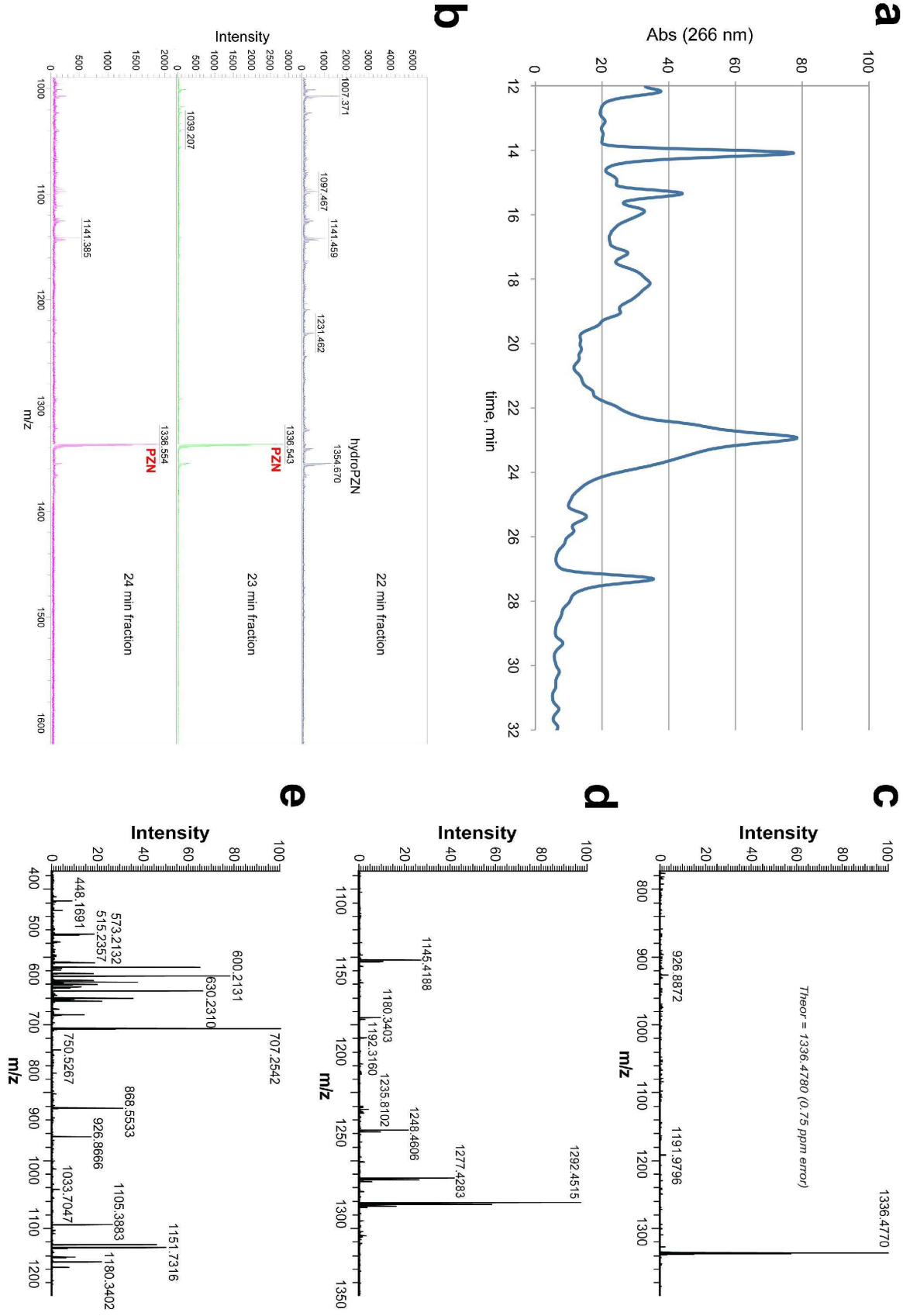
a
Abs (266 nm)
time, min
b
Intensity
m/z
1007.371
1097.467
1141.459
1231.462
1354.670
hydroPZN
22 min fraction
1039.207
1336.543
PZN
23 min fraction
1141.385
1336.554
PZN
24 min fraction
c
Intensity
m/z
Theor = 1336.4780 (0.75 ppm error)
926.8872
1191.9796
1336.4770
d
Intensity
m/z
1145.4188
1180.3403
1192.3160
1235.8102
1248.4606
1277.4283
1292.4515
e
Intensity
m/z
448.1691
515.2357
573.2132
600.2131
630.2310
707.2542
750.5267
868.5533
926.8666
1033.7047
1105.3883
1151.7316
1180.3402

(PREVIOUS PAGE) Demonstration of PZN production from *Bacillus pumilus* ATCC 7061. Cells were grown in an identical fashion to *B. amyloliquefaciens*. **A**, The cell surface metabolites were extracted with methanol, dried, concentrated, and separated on a preparative C_{18}-HPLC column with UV monitoring at 266 nm (λ_{max} for PZN). **B**, The 22-min (top), 23-min (middle), and 24-min (bottom) fractions from HPLC purification were concentrated and spotted on to the MALDI target with sinapic acid. In the earliest fraction, m/z 1354 (hydrolyzed PZN is visible). In the latter two fractions, m/z 1336 (PZN) is readily identified, which was pooled for further analysis. **C**, HPLC purified PZN from *B. pumilus* was subjected to high-resolution MS (LTQ-FT-MS), which verified the molecular formula to be consistent with PZN within the mass accuracy of the instrument (<5 ppm). **D**, CID spectrum obtained upon isolation of the singly charged (*m/z* 1336) precursor ion. This data is analogous to Fig 1b (PZN from *B. amylo.* RSpMarA2). Fig 1b. **E**, CID spectrum obtained upon isolation of the doubly charged (*m/z* 668) precursor ion. This data is analogous to Fig S1b (PZN from *B. amylo.* RSpMarA2). However, different instrumental settings had to be employed to visualize the PZN ions, which were less abundant than from the *B. amylo*. overproducer (RSpMarA2) and required summing over many scans. An unidentified contaminant and instrumental noise account for the ions between *m/z* 750-1100.

Supporting references

1. Lee, S. W., Mitchell, D. A., Markley, A. L., Hensler, M. E., Gonzalez, D., Wohlrab, A., Dorrestein, P. C., Nizet, V., and Dixon, J. E. (2008) Discovery of a widely distributed toxin biosynthetic gene cluster, *Proc Natl Acad Sci U S A 105*, 5879-5884.
2. Scholz, R., Molohon, K. J., Nachtigall, J., Vater, J., Markley, A. L., Sussmuth, R. D., Mitchell, D. A., and Borriss, R. (2011) Plantazolicin, a novel microcin B17/streptolysin S-like natural product from Bacillus amyloliquefaciens FZB42, *J Bacteriol 193*, 215-224.
3. Frump, J. A. (1971) Oxazolines - Their Preparation, Reactions, and Applications, *Chemical Reviews 71*, 483-&.